Fermi National Accelerator Laboratory

FERMILAB-Pub-90/59-E
[BNL E-840]

Measurement of the Magnetic Birefringence of Neon Gas*

R. Cameron, G. Cantatore, A. C. Melissinos, J. Rogers, and Y. Semertzidis
University of Rochester
Rochester, New York 14627

H. Halama and A. Prodell
Brookhaven National Laboratory
Upton, New York 11973

F. A. Nezrick
Fermi National Accelerator Laboratory
P.O. Box 500
Batavia, Illinois 60510

C. Rizzo
INFN, Sezione Trieste, Via Valerio 2,
34127 Trieste, Italy

E. Zavattini
Universita di Trieste, Via Valerio 2,
34127 Trieste, Italy

April 1990

* Submitted to the Journal of the Optical Society of America B.

Measurement of the Magnetic Birefringence of Neon Gas

R. Cameron, G. Cantatore, A. C. Melissinos,
J. Rogers† and Y. Semertzidis
Department of Physics and Astronomy
University of Rochester
Rochester, NY 14627

H. Halama and A. Prodell
Brookhaven National Laboratory
Upton, NY 11973

F. A. Nezrick
Fermi National Accelerator Laboratory
Batavia, IL 60510

C. Rizzo
INFN Sezione Trieste, Via Valerio 2,
34127 Trieste, Italy

E. Zavattini
Dipartimento di Fisica
Universita di Trieste
Via Valerio 2, 34127 Trieste, Italy

(Submitted to the Journal of the Optical Society of America B)

† Present address: Brookhaven National Laboratory, Upton, NY 11973

Abstract

We have constructed a sensitive ellipsometer to study very small ellipticities acquired by laser light traversing a multipass optical cavity in a $9\,m$ long superconducting magnet. This set-up has been used to measure the Cotton-Mouton constant of Neon at 514.5 nm. We find for 1 atmosphere and $25°C$ and that $C_{CM}(Ne) = (5.5 \pm 0.3) \times 10^{-20}$ Gauss$^{-2} cm^{-1}$.

1. Introduction

We present the first measurement of the Cotton-Mouton constant of Neon gas, in the pressure range from 20-200 *torr* and at $\lambda = 514.5nm$.

The Cotton-Mouton (CM) effect[1] refers to the birefringence induced in a gas by a magnetic field. The constant C_{CM} is defined by

$$\Delta n = n_p - n_n = C_{CM}\lambda B^2 \ , \tag{1}$$

where $n_p(n_n)$ is the refractive index for light polarized parallel (normal) to the magnetic field, B is the component of the magnetic field normal to the direction of propagation of the light, at wavelength λ. The difference in the refractive indices can be determined by measuring the ellipticity ψ acquired by linearly polarized light after traversing the medium in the presence of the magnetic field

$$\psi = \frac{\pi L}{\lambda}\,\Delta n = \pi C_{CM} \sin 2\theta \int \left(\vec{B} \times \vec{k}\right)^2 dx \ , \tag{2}$$

where L is the total optical path length, $\vec{k}$ is the light propagation vector, and θ is the angle between $\vec{B} \times \vec{k}$ and the polarization (electric field) vector of the light. The integration is carried over the length of the optical path.

In our set-up we use an Argon ion laser ($\lambda = 514.5\,nm$) and two 4.5 m long superconducting dipoles.[2] The polarization is at 45° with respect to the direction of the magnetic field, which is amplitude modulated at a frequency of $78.125\,mHz$. The induced ellipticity is converted to an optical rotation by a quarter-wave ($\lambda/4$) plate and mixed with the rotation signal of a Faraday cell driven at a frequency of 260 Hz. In this way the signal depends on the amplitude of the Cotton-Mouton effect (rather than on its square) and is displaced from the zero Hz region. The sensitivity achieved with this set-up, excluding systematic effects is an ellipticity

$$\psi = 1.0 \times 10^{-8}/\sqrt{Hz} \ .$$

We investigated N_2 and Ne and measured their Cotton-Mouton constants. Experimental values for Nitrogen have been previously determined[3,4] while for Neon only upper bounds exist[5]. We intend to extend our measurements to other gases in the near future.

2. Experimental Apparatus

A schematic drawing of the apparatus is shown in Fig. 1. Linearly polarized light from a continuous wave Argon ion laser (Coherent Inc., Palo Alto, CA; Mod. Innova 90) at $514.5\,nm$ is directed by the periscope PS and the mirror $M1$ through the glass window $W1$ into a vacuum enclosure. The laser is operated at 0.5 W single line power. The optical components are housed in an aluminum vacuum box which is directly connected to the multipass optical cavity. Windows are anti-reflection coated and slightly tapered to prevent interference of multiple reflections from their two surfaces.

The entrance polarizing prism P (Karl-Lambrecht Corp., Chicago, IL; Mod. MGLQD-12V515) is oriented at 45° with respect to the vertical. The half-wave plate HWP is used to rotate the intial polarization of the beam to coincide with the polarizer axis. After the polarizer the light passes through a hole in the center of mirror $M2$ and enters the optical cavity. The latter consists of two dielectric multilayer interferometric mirrors[6], 11.25 cm in diameter, focal length 950 cm, and separated by a distance of 1256 cm; the reflectivity was better than 99.8 %. The entrance mirror had a 5.7 mm hole at its center. After multiple reflections the light beam exits the cavity through the same hole[7]. For the measurements reported here the light made 36 passes in the cavity, for other measurements we have achieved in excess of 500 traversals by slightly deforming one of the mirrors[8]. The telescope TL is necessary to match the laser beam to the optical cavity[9].

Upon exiting the cavity, the light beam is reflected by mirror $M2$ towards the spherical mirror $M3\,(f = 2m)$ which focuses the beam through the $\lambda/4$ plate QWP and the Faraday cell FC onto the analyzing prism A. The $\lambda/4$ plate is aligned for maximum extinction in the absence of the magnetic field; thus the induced ellipticity is converted to an optical rotation which mixes with the rotation introduced by the Faraday cell. The Faraday

cell consists of a 1.27 cm diameter, 2.54 cm thick $BK7$ optical flat placed in a solenoid such that the rotation coefficient is $8.26 \times 10^{-5}\ rad/V$. The analyzing prism A (Karl-Lambrecht Corp., Chicago, IL; Mod. MGLQD-12V515) is crossed with P for maximum extinction. The transmitted light passes through the window $W2$ and is focussed by the lens L onto a $1\ mm^2$ silicon photodiode PD (Hamamatsu, Bridgewater, NJ; Mod. S1336-18BQ). Typical extinction factors, obtained after compensating residual static ellipticities by properly orienting the cavity mirrors and rotating the Faraday cell glass around its horizontal axis, were of the order of 10^{-7}. All optical surfaces were antireflection coated; the entrance and exit surfaces of the polarizing prisms had a 3° slant angle to prevent interference between multiple reflections.

The two superconducting magnets[10] establish a highly uniform vertical dipole field over an aperture of 8.8 cm. They are fitted with a 7 cm diameter stainless steel warm bore beam pipe which was part of the optical cavity. The cavity could be evacuated to a pressure of 10^{-7} $torr$. The effective length of the field region was 880 cm, and the field amplitude was modulated from 1.94 T to 2.48 T with a 12.8 s period. The induced ellipticity is proportional to the optical path length L where $L = \ell N$, ℓ is the effective length of the magnetic field region, and N the number of passes of the light through the cavity.

The electronics layout is shown in Fig. 2. The current from the photodiode was amplified and converted to a voltage signal by a preamplifier (EG&G, Bedford, MA; Mod. 181) with a $10^8\Omega$ input impedance. This was followed by a passband filter (Frequency Devices Inc., Haverhill, MA; Mod. 9002) set between 120 Hz and 300 Hz to reject the DC and 520 Hz components of the signal. The frequency power spectrum of the signal (both amplitude and phase) centered at 260 Hz was then obtained with 4 mHz resolution from a Hewlett Packard Mod. 35660A Fast Fourier Transform (FFT) signal analyzer. The built-in frequency synthesizer of the FFT provided the 260 Hz sine wave input signal to the power amplifier (Crown Inc., Elkhart, IN; Techron Mod. 5515) driving the Faraday

cell coil. The same 260 Hz signal, after being scaled down, generated a TTL pulse train at 78.125 mHz which triggered the magnetic field modulation and the signal analyzer trigger.

The data from the signal analyzer were transferred through the $HPIB$ interface to a PC (Personal Computer, Dell Corp., Austin, TX; Mod. 286) which stored them and displayed a running vector average of the signal power spectra. The PC was also used to control the settings and functions of the signal analyzer and, between runs, to adjust the optics for optimum extinction. All critical optical elements were computer controlled via an "Encoder Mike Controller" (Oriel Corp., Stratford, CT; Mod. 18011).

3. Method and Data Analysis

The light power incident on the photodiode can be written as

$$W(t) = W_0 \left\{ \sigma^2 + [\eta(t) + \psi(t) + \alpha(t)]^2 + \Gamma^2(t) \right\} \tag{3}$$

where

W_0 is the light power before the analyzing prism, typically $10 - 50\, mW$;

σ^2 is the extinction factor; as mentioned previously typically $\sigma^2 \sim 10^{-7}$;

$\eta(t) = \eta_0 \cos(2\pi f_F t + \phi_F)$ is the rotation angle introduced by the Faraday cell: the data were obtained with $\eta_0 = 6.95 \times 10^{-4}\, rad$ and $f_F = 260\, Hz$;

$\psi(t)$ is the effect to be measured. In view of the periodic modulation of the magnetic field, $\psi(t)$ can be expressed by a Fourier series

$$\psi(t) = \sum_{n=0}^{\infty} \psi_n \cos(2\pi n f_M + \phi_n)$$

with

$$f_M = 78.125\, mHz \quad .$$

$\alpha(t)$ is the residual misalignment angle between polarizing and analyzing prisms and is of order 10^{-6};

$\Gamma(t)$ is an incoherent time dependent noise signal, including any residual uncompensated ellipticity.

The amplitudes $\alpha(t)$ and $\Gamma(t)$ drift slowly over a magnet period and ψ_n, $\alpha(t)$, $\Gamma(t) \ll \eta_0$, so the signal at the output of the preamplifier can be written to sufficient accuracy as

$$\begin{aligned} V(t) =& \mu R W_0 \Big\{ \sigma^2 + \frac{{\eta_0}^2}{2} + 2\alpha\eta_0 \cos\left(2\pi f_F + \phi_F\right) \\ &+ \eta_0 \sum_{n=0}^{\infty} \psi_n \cos\left[2\pi(f_F - nf_M)t + (\phi_F - \phi_n)\right] \\ &+ \eta_0 \sum_{n=0}^{\infty} \psi_n \cos\left[2\pi(f_F + nf_M)t + (\phi_F + \phi_n)\right] + \frac{{\eta_0}^2}{2} \cos\left[4\pi f_F t + 2\phi_F\right] \Big\} \end{aligned} \tag{4}$$

where $\mu = 0.27\ A/W$ is the diode quantum efficiency and $R = 10^8\ \Omega$ is the preamplifier input impedance. Table 1 lists the relevant spectral components of the signal indicated by Eq. (4); in this notation the amplitude of the spectral components of the ellipticity $\psi(t)$ is

$$\psi_n = \frac{\eta_0 I_{n+}}{2I_{2\omega_F}} = \frac{\eta_0 I_{n-}}{2I_{2\omega_F}} \tag{5}$$

and their phase

$$\phi_n = \frac{1}{2}\left(\phi_{n+} - \phi_{n-}\right) \ . \tag{6}$$

Data were taken in records of 256 s duration with a resolution of 3.90625 mHz over a 400 channel spectrum centered at the carrier frequency of 260 Hz. When the record was completed, a wideband spectrum (total width 800 Hz) was obtained to record the amplitudes at 0 Hz and 520 Hz as well. This was followed by an automatic minimization of the misalignment angle. The data were stored on disk and later transferred to a VAX computer for off-line analysis. Typically 10 to 20 records were taken for every gas/pressure point.

The magnetic field modulation is shown in the time domain in Fig. 3(a) and its directly measured Fourier spectrum in Fig. 3(b). The ramping rate was 115 A/s between 1.25 kA and 1.6 kA corresponding[11] to 1.94 T and 2.48 T, and the cycle period was 12.8 s. From Fig. 3(b) we note that the dominant component is at the first harmonic. Fig. 4 shows a typical power spectrum of the signal obtained from N_2 gas. The spectrum shown is a vector average of 20 records each of 256 s duration. The peak appearing at 260 Hz

is due to the misalignment angle while the sidebands are the harmonics of the modulated ellipticity in exact correspondence with the Fourier spectrum of the magnetic field shown in Fig. 3(b).

To extract the CM constant it suffices to use the first harmonic. From each record we obtain I_1 and ϕ_1 and then calculate the amplitude ψ_1 using Eq. (5); η_0 is known from both the Faraday cell calibration and a direct measurement of the DC component. $I_{2\omega_F}$ is measured just before and after the record is taken. The values of ψ_1 are averaged over all records corresponding to the same data point, i.e. gas and pressure, to yield $\bar{\psi}(P)$. Since at these pressures one expects the ellipticity induced by the CM effect to be proportional to the density we have fitted to the data the expression

$$\bar{\psi}(P) = aP + b \tag{7}$$

where P is the pressure. The results of the fit for N_2 and Ne gas are given in Table II, where a is the ellipticity (at the first harmonic) per unit pressure and b is an intercept, which in principle should be zero. The quality of the least squares fit is expressed as χ^2 per degree of freedom (DF).

To find the CM constant we use the value of a determined from the fit in Eq. (2); the integral over the field has been taken as $2B_0\Delta B\ell N$ since only the time-dependent component of B^2 contributes. Here $\ell = 880\,cm$ is the total effective length of the field region and $N = 36$ is the number of passes in the optical cavity. B_0 is the mean field value and ΔB is the modulation amplitude;

$$B_0 = \frac{1}{2}\,(B_{\max} + B_{\min}) \quad , \quad \Delta B = \frac{1}{2}\,(B_{\max} - B_{\min}) \quad . \tag{8}$$

To account for the fact that a is obtained from the first harmonic, we use the corresponding values from the zeroth and first harmonic of the magnetic field

$$B_0 = 2.18\,T \quad , \quad \Delta B = 0.31\,T \ . \tag{9}$$

The data were taken at a temperature $T = 25°C$ and are referenced to 760 $torr$, so that

$$C_{CM} = a \frac{760}{2\pi N \ell B_0 \Delta B} \frac{1}{\sin 2\theta} \quad , \tag{10}$$

with $\theta = 45°$.

In our set-up all frequencies are derived from the internal source of the signal analyzer so that the Faraday cell modulation, the magnet modulation, and the reference of the power spectrum are phase locked. Thus the phase of the first harmonic directly determines the sign of C_{CM} for Neon relative to that of Nitrogen.

4. Results and Discussion

The values of $\bar{\psi}(P)$ for Nitrogen and Neon are shown as a function of gas pressure in Figs. 5 and 6 respectively. The N_2 gas was 99.996% pure and the Ne gas was 99.995% pure with O_2 content less than 3.0 ppm and H_2O content less than 5.0 ppm. Such purity is necessary since the CM constant of O_2 is $-4.89 \times 10^{-16}\text{Gauss}^{-2}\ cm^{-1}$, four orders of magnitude larger than that of Ne.

The magnetic field amplitude and the effective length of the field region are known to better than one percent[11], while the number of passes in the cavity was determined by counting the spots visible on each cavity mirror. Thus the relative error on the factor $N\ell B_0 \Delta B$ in Eq. (10) is taken as ± 0.01. Considering other effects such as the error in the angle θ between the field direction and the light polarization we assign an overall systematic error of ± 0.02. This error is combined in quadrature with the statistical error on a obtained from the fit as shown in Table II. The final error on the C_{CM} shown in the last column of the Table is the quadrature of the two effects.

Our result for Nitrogen

$$C_{CM}(N_2) = -(4.4 \pm 0.2) \times 10^{-17}\ \text{Gauss}^{-2} cm^{-1}$$

is in good agreement with that of Ref. (5) where $C_{CM}(N_2, T = 0°C) = -(5.1 \pm 0.3) \times 10^{-17}\,(\text{Gauss})^{-2} cm^{-1}$; since our result is at $T = 25°C$ the result of Ref. (5) must be scaled

as T^{-2} (see Ref. (3)) yielding $C_{CM}(N_2, T = 25°C) = -(4.3 \pm 0.2) \times 10^{-17}$ Gauss$^{-2}cm^{-1}$. Our new result for Neon is

$$C_{CM}(Ne) = (5.5 \pm 0.3) \times 10^{-20} \text{ Gauss}^{-2}cm^{-1} \quad .$$

While there exists no exact calculation for $C_{CM}(Ne)$ a simple model discussed in Ref. (12) relates the CM constant to the radius of the first excited level of Neon; from our data we find for the radius $\sqrt{< r_1^2 >} = 1.87$ $\mathring{A}$, in good agreement with expectation.

The intercepts b obtained for both Nitrogen and Neon are very similar and of the same order as observed with the cavity evacuated to 10^{-7} $torr$. Thus they indicate the presence of a systematic ellipticity induced by the apparatus at the level of 1 to 2×10^{-8}. While this background does not affect in any way the present data, it must be eliminated if one wishes to measure much smaller ellipticities, such as that induced by the birefringence of the vacuum[13].

It is a pleasure to acknowledge the generous support of Brookhaven National Laboratory and in particular of the ADD Magnet Division that made these measurements possible. We thank J. Briggs, G. Ganetis, H. Hildebrand and R. Meier for the installation and operation of the magnet system; T. Blair, A. Penzick and J. Scaduto provided expert technical coordination. We also thank Dr. D. Lazarus and Mr. T. Park for help in running the experiment. This work was supported in part by the U.S. Department of Energy under contracts DE-AC02-76ER13065, DE-AC02-76CH03000, and DE-AC02-76CH00016.

References and Notes

1. See for instance Handbook of Optics section 17-21 W. G. Driscoll and W. Vaughan Eds. McGraw Hill, NY 1958.
2. The dipole magnets were originally constructed for the Colliding Beam Accelerator project at Brookhaven National Laboratory, Upton, N.Y. 11973.
3. A. D. Buckingham, W. H. Prichard, and D. H. Whiffen, Trans. Far. Soc., 63, 1057 (1967).
4. S. Carusotto, E. Iacopini, E. Polacco, G. Stefanini, and E. Zavattini, Opt. Commun. 42, 104 (1982).
5. S. Carusotto et al., J. Opt. Soc. Am. 1B, 635 (1984).
6. The mirrors were ground by Optical Prototypes Inc., Rochester, N.Y. and coated by the Laboratory of Laser Energetics of the University of Rochester.
7. D. Herriot, H. Kogelnik, R. Kompfner, Appl. Opt. 3, No. 4 (1964).
8. D. Herriot, H. J. Schulte, Appl. Opt., 4, No. 8, (1965).
9. H. Kogelnik, T. Li, Proc. IEEE, 54, No. 10 (1966).
10. CBA Magnets LM0014 and LM0018 see E. J. Bleser et al., Nucl. Instr. and Meth. in Phys. Res. A235, 435 (1985).
11. Brookhaven National Laboratory, Magnet Division, Test and Measurement Group notes TMG-259, 12/16/89; TMG-270, 2/7/83.
12. F. Scuri et al., J. Chem. Phys. 85, 1789 (1986).
13. E. Iacopini and E. Zavattini, Phys. Lett. 85B, 151 (1979).

Figure Captions

Fig. 1 Schematic drawing of the experimental set-up and optical path.

Fig. 2 Schematic of the electronics and data acquisition system.

Fig. 3 The magnetic field modulation cycle. (a) Magnet excitation current vs time, (b) power spectrum of the excitation current. The DC amplitude is 9.1 dBV.

Fig. 4 Signal power spectrum for N_2 at a pressure $P = 250\, mtorr$. The central frequency is 260 Hz and the full width of the spectrum is 1.5625 Hz. With 400 channels the resolution is 3.90625 mHz/channel.

Fig. 5 The averaged ellipticity $\bar{\psi}(P)$ at the first harmonic for N_2 gas as a function of pressure in $torr$. The straight line is a least square fit to the data. The vertical bars are an estimate of the statistical error at each point.

Fig. 6 Same as Fig. 5 but for Ne gas.

Table I

Fourier components of the photodiode signal.

Frequency (Hz)	Fourier Component	Amplitude	Phase
0	DC	$\sigma^2 + \frac{\eta_0^2}{2}$	—
260	I_{ω_F}	$2\ \alpha\eta_0$	ϕ_F
$260.0 + nf_M$	I_{n+}	$\psi_n\eta_0$	$\phi_F + \phi_n \equiv \phi_{n+}$
$260.0 - nf_M$	I_{n-}	$\psi_n\eta_0$	$\phi_F - \phi_n \equiv \phi_{n-}$
520	$I_{2\omega_F}$	$\frac{\eta_0^2}{2}$	$2\phi_F$

Table II

Summary of experimental results.

Gas	$a(torr^{-1})^*$	b	χ^2/DF	C_{CM} (Gauss$^{-2}cm^{-1}$)**
N_2	$(7.8 \pm 0.3) \times 10^{-7}$	$(1.7 \pm 0.8) \times 10^{-8}$	.7/1	$(-4.4 \pm 0.2) \times 10^{-17}$
Ne	$(9.8 \pm 0.4) \times 10^{-10}$	$(1.3 \pm 0.5) \times 10^{-8}$	8.6/4	$(5.5 \pm 0.3) \times 10^{-20}$

* a and b derived from fitting $\bar{\psi}(P) = aP + b$ to the data.

**C_{CM} at $P = 760\,torr$ and $T = 25°C$.

Figure 1.

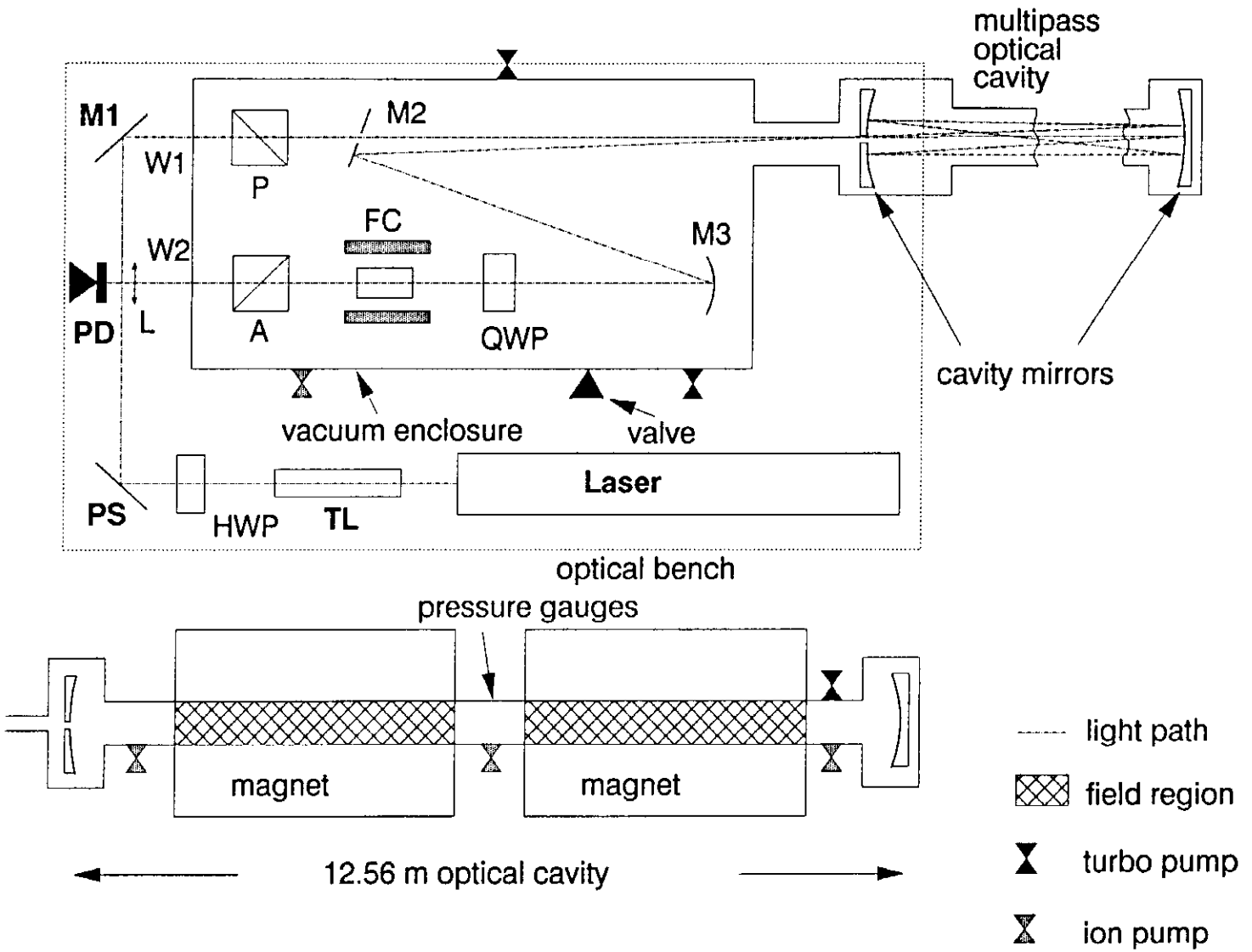
multipass
optical
cavity
M1
M2
W1
P
FC
M3
W2
PD
L
A
QWP
cavity mirrors
vacuum enclosure
valve
Laser
PS
HWP
TL
optical bench
pressure gauges
magnet
magnet
12.56 m optical cavity
light path
field region
turbo pump
ion pump

Figure 2.

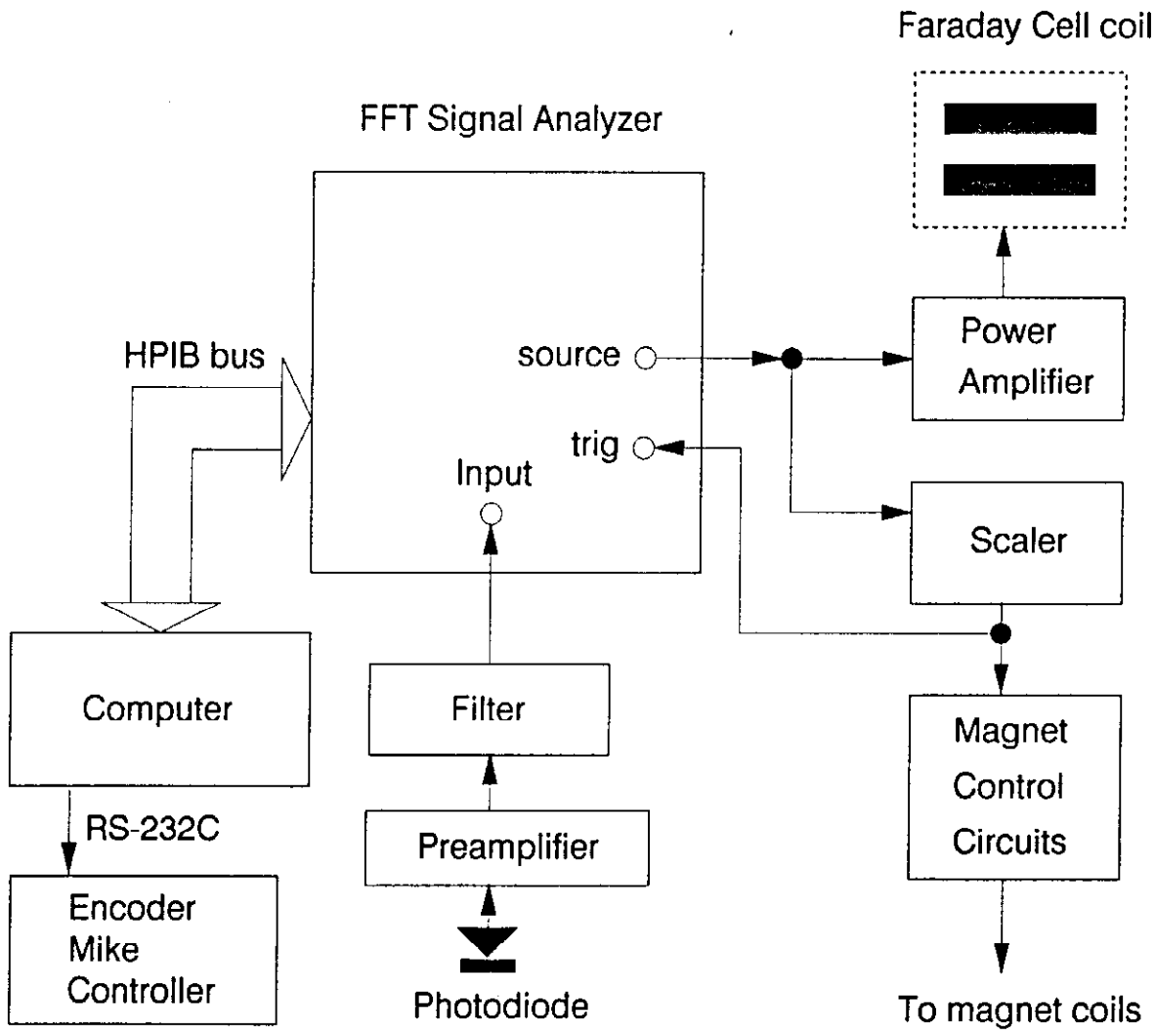
Faraday Cell coil
FFT Signal Analyzer
HPIB bus
source
trig
Input
Power
Amplifier
Scaler
Computer
Filter
Magnet
Control
Circuits
RS-232C
Preamplifier
Encoder
Mike
Controller
Photodiode
To magnet coils

Figure 3a.

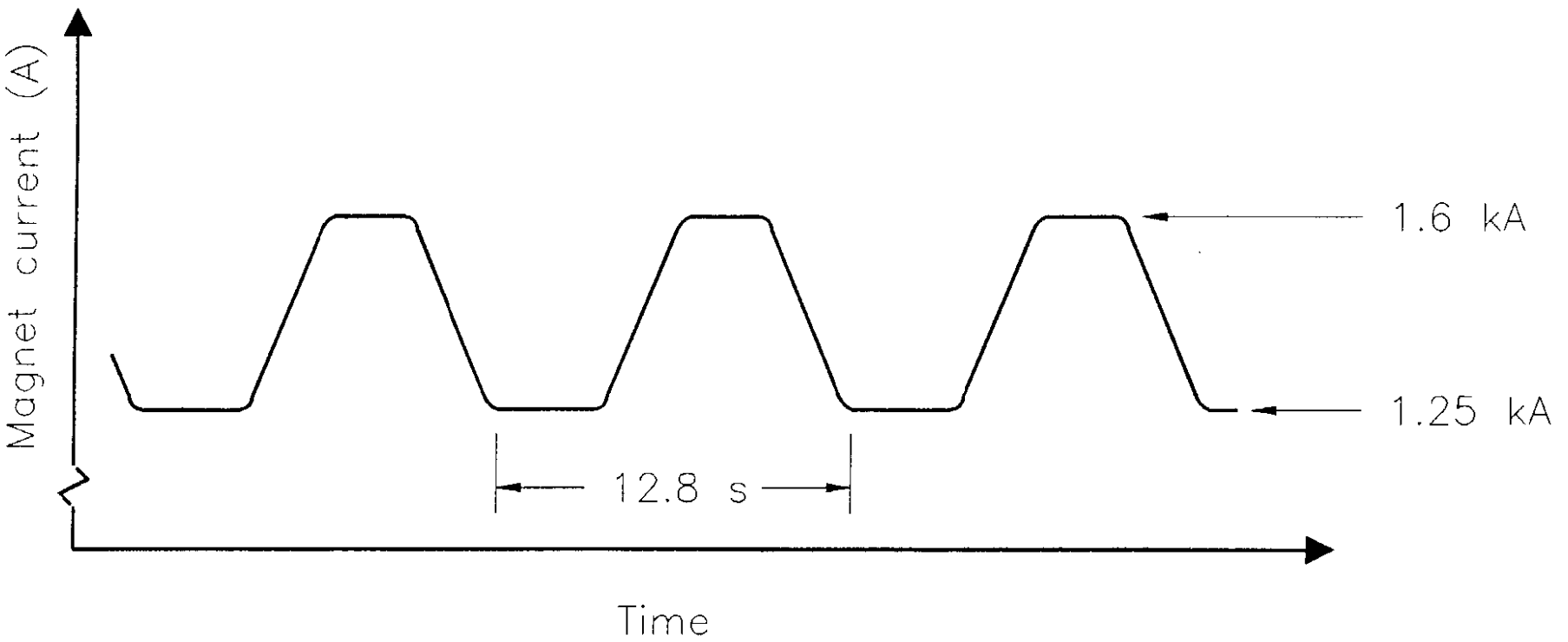

Figure 3b.

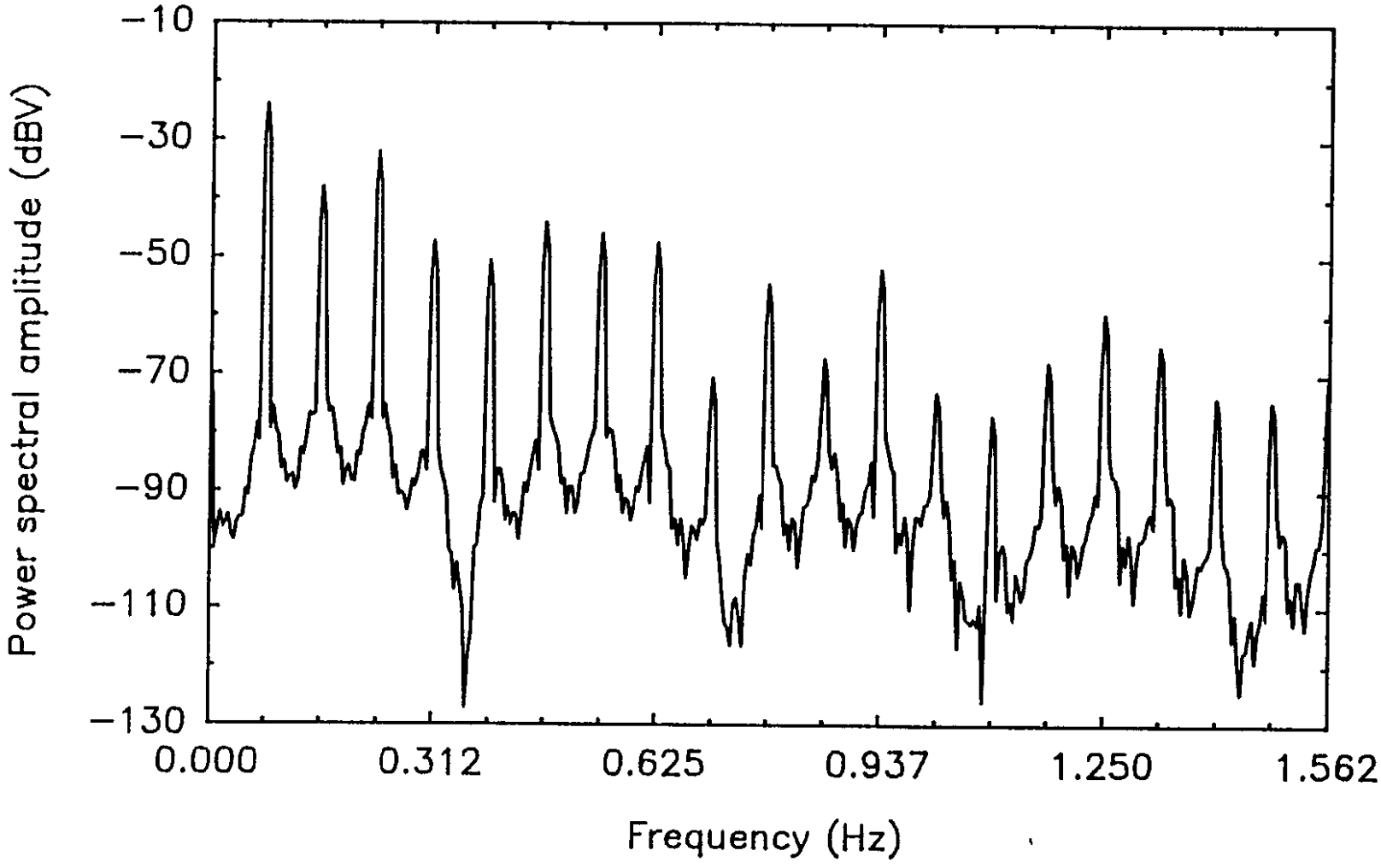
-10
-30
-50
-70
-90
-110
-130
Power spectral amplitude (dBV)
0.000
0.312
0.625
0.937
1.250
1.562
Frequency (Hz)

Figure 4.

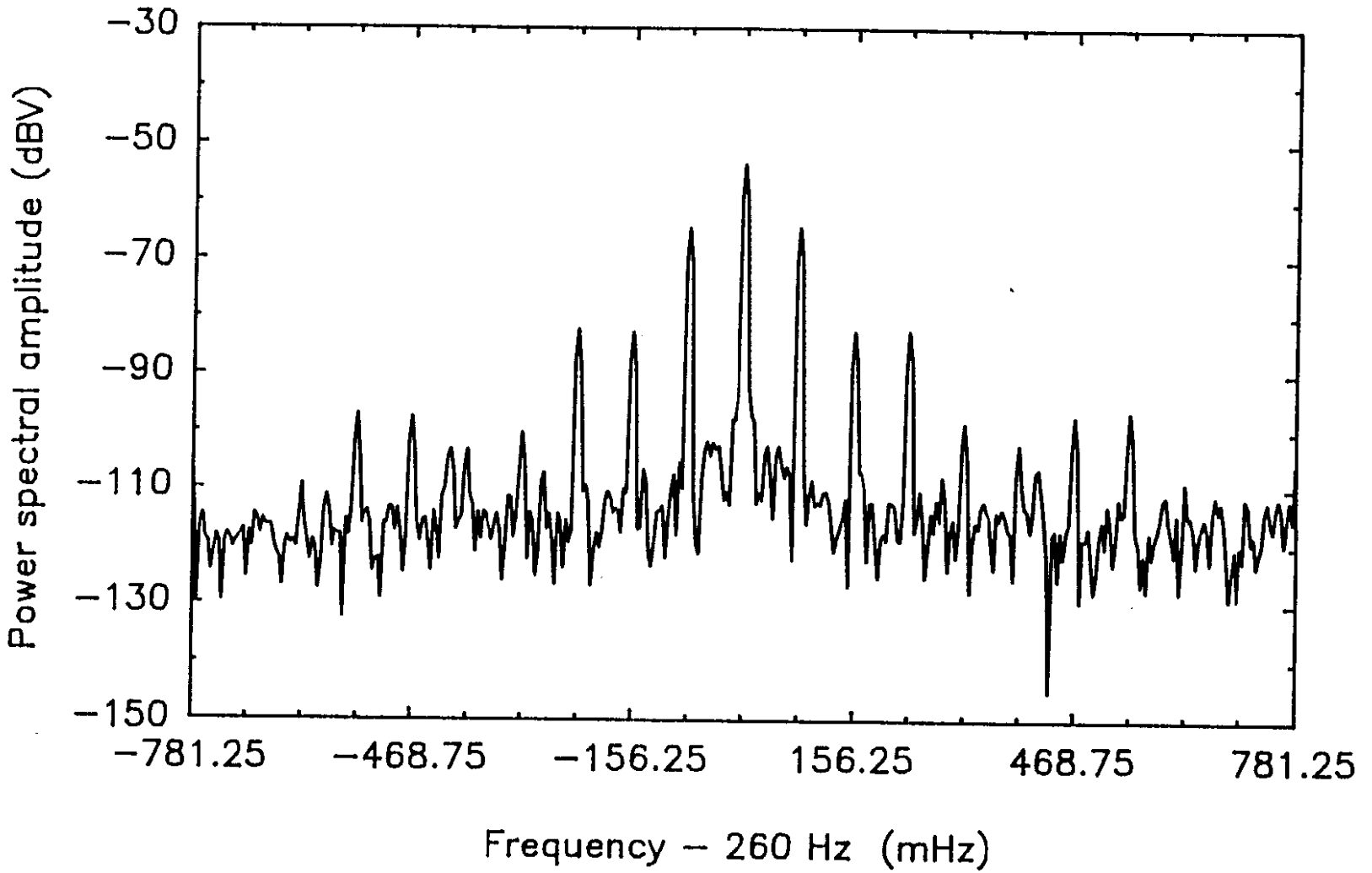
−30
−50
−70
−90
−110
−130
−150
Power spectral amplitude (dBV)
−781.25
−468.75
−156.25
156.25
468.75
781.25
Frequency − 260 Hz (mHz)

Figure 5.

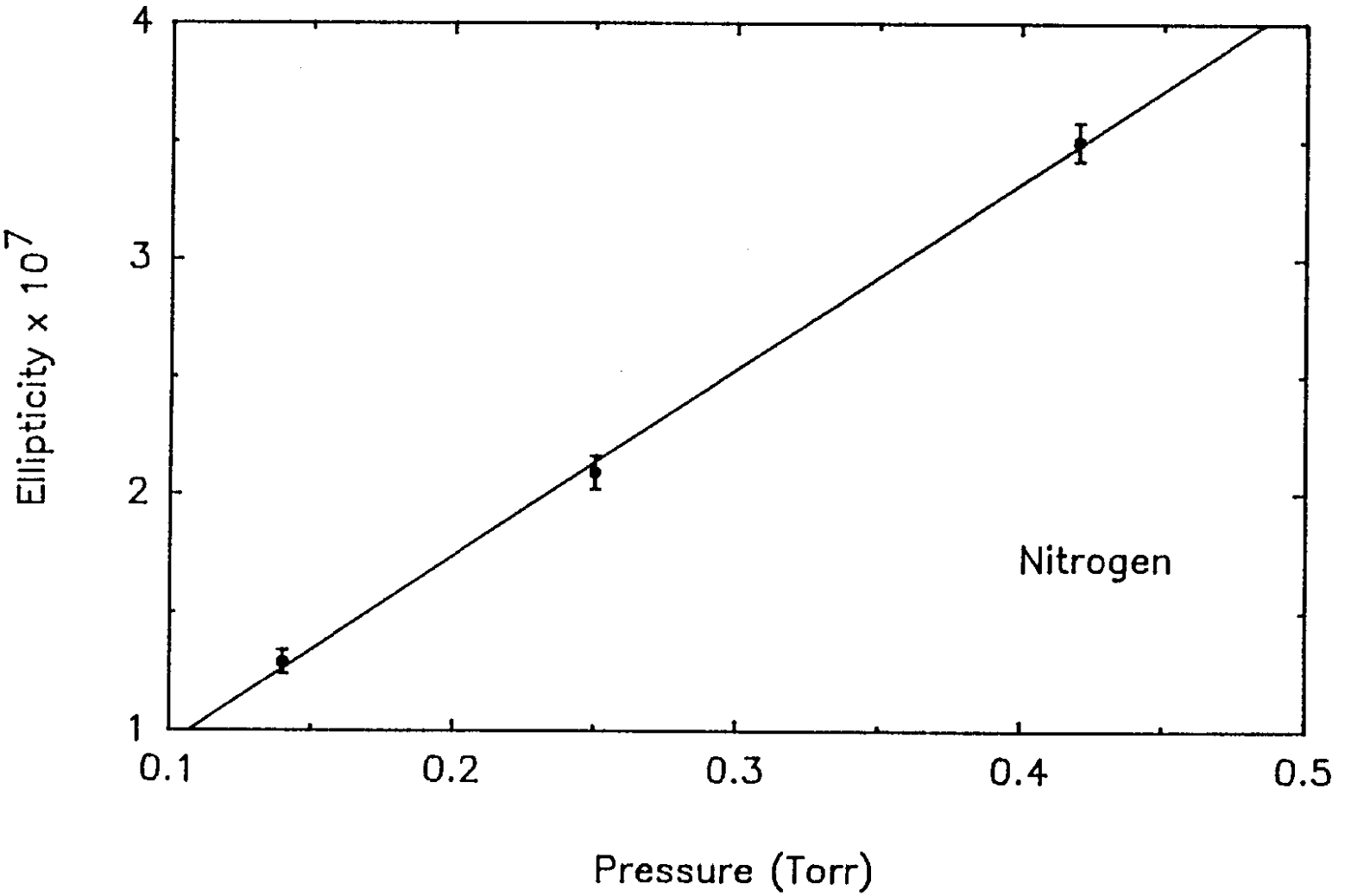

Figure 6.

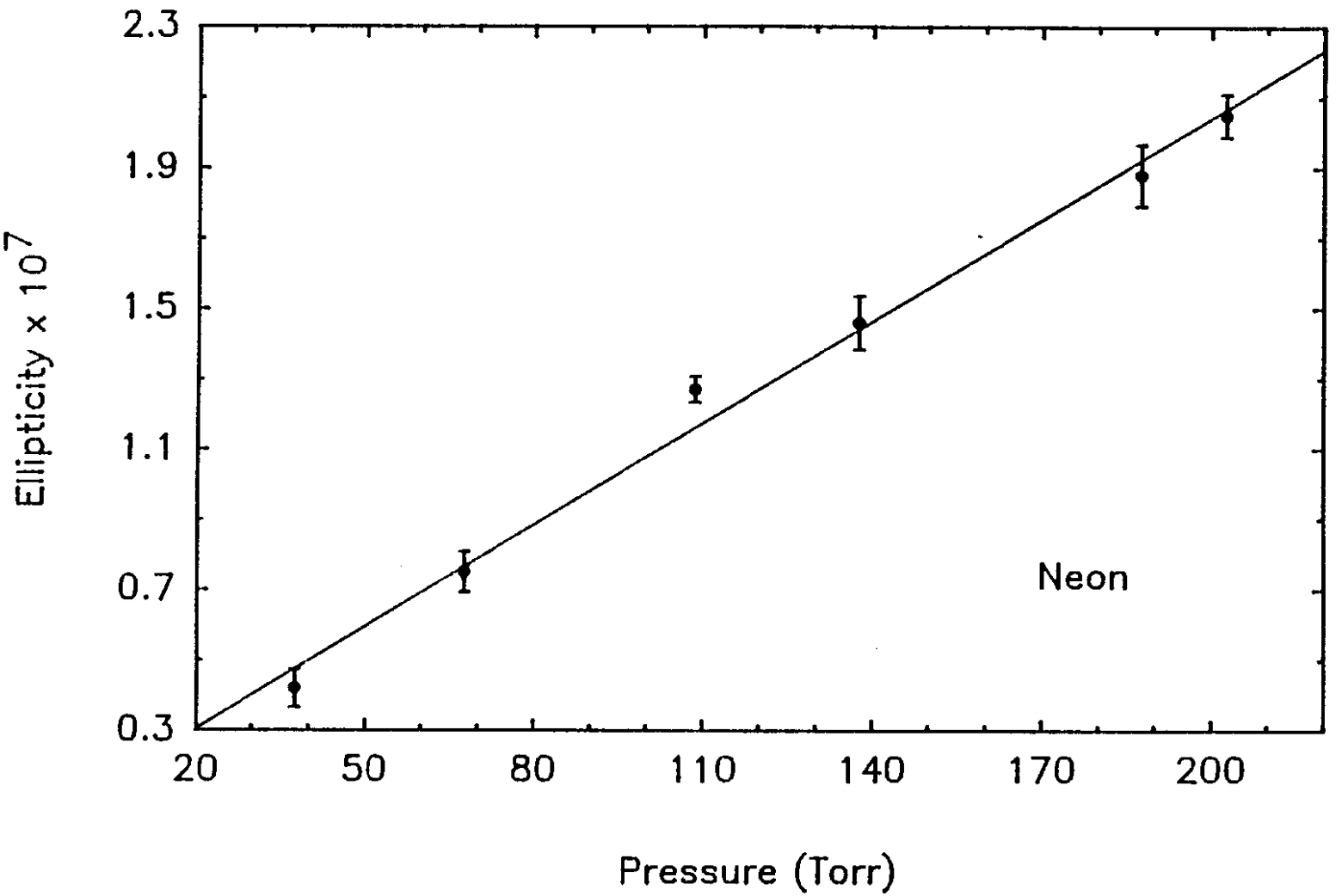
2.3
1.9
1.5
1.1
0.7
0.3
Ellipticity x 10^7
20
50
80
110
140
170
200
Pressure (Torr)
Neon